Revista de Metalurgia
October-December 2022, 58 (4), e230
ISSN-L: 0034-8570
https://doi.org/10.3989/revmetalm.230

Microstructure and mechanical properties on friction stir processed TIG welded dissimilar joints of AA5052-H32 and AA5083-H111 alloys by grey approach

Chandrasekaran Chanakyan[a,*], Dhanaraj Antony Prabu [b], Sivasamy Alagarsamy[c], Mark Martin Charles[b]

[a] Assistant Professor, Department of Mechanical Engineering, R. V. S. College of Engineering and Technology, Kumarankottam Campus, Coimbatore, Tamilnadu, India

[b] Assistant Professor, Department of Mechanical Engineering, Loyola-ICAM College of Engineering and Technology (LICET), Chennai, Tamilnadu, India

[c] Assistant Professor, Department of Mechanical Engineering, Mahath Amma Institute of Engineering and Technology, Pudukkottai, Tamilnadu, India

(*Corresponding author: chanmech89@gmail.com)

Submitted: 4 July 2022; Accepted: 24 November 2022; Available On-line: 27 December 2022

ABSTRACT: In this investigation, the mechanical behaviour and microstructural examination of friction stir processed (FSP) Tungsten Inert Gas (TIG) welded aluminium dissimilar alloys has been studied. The research is proposed to enhance the mechanical characteristics of the aluminium alloy 5052-H32 and aluminium alloy 5083-H111 TIG FSP welded joints. Initially, the TIG welding was done to join aluminium alloy 5052-H32 and aluminium alloy 5083-H111 by employing a ER5356 filler rod. TIG welding is performed by using the following parameters: tungsten electrode diameter (2.4 mm), Current (170 A) and a shielding gas flow rate (argon) (11 $l{\cdot}min^{-1}$). Secondarily, the FSP is carried out on TIG welded aluminium alloy 5052-H32 and aluminium alloy 5083-H111 by using different tool rotation speeds (850 to 1050 rpm), tool traverse speeds (24 to 32 $mm{\cdot}min^{-1}$) and different number of passes (1 to 3) with a cylindrical pin less tool. The FSP parameters are designed by the Taguchi L9 array to compute the optimized parameters. The tensile strength, microhardness and % of elongation are determined for a total of nine specimens. Finally, the grey relational analysis (GRA) is employed to find out the best FSP parameter out of the set of FSP parameters. The optimal parameters of FSP are a tool rotation speed of 950 rpm, tool traverse speed of 28 mm/min and number of passes of 3. The number of passes are the most influencing factor when compared to other two FSP parameters.

KEYWORDS: Aluminium alloys; Electron Microscopy; Friction stir processing; Grey relational analysis; Scanning Tensile testing; TIG welding

Citation/Citar como: Chanakyan, C.; Antony Prabu, D.; Alagarsamy, S.V.; Martin Charles, M. (2022). “Microstructure and mechanical properties on friction stir processed TIG welded dissimilar joints of AA5052-H32 and AA5083-H111 alloys by grey approach”. *Rev. Metal.* 58(4): e230. https://doi.org/10.3989/revmetalm.230

RESUMEN: *Microestructura y propiedades mecánicas en uniones disimilares soldadas por TIG y procesadas por soldadura por fricción-agitación de las aleaciones AA5052-H32 y AA5083-H111 utilizando un análisis relacional gris.* En esta investigación, se estudió el comportamiento mecánico y se realizó un estudio microestructural de aleaciones disímiles de aluminio soldadas con gas inerte de tungsteno (TIG) y posteriormente soldadas por fricción-agitación (FSP). La investigación propone mejorar las características mecánicas de las uniones soldadas TIG-FSP de las aleaciones de aluminio 5052-H32 y 5083-H111. Inicialmente, la soldadura TIG se realizó para unir la aleación de aluminio 5052-H32 y la aleación de aluminio 5083-H111 mediante el empleo de una varilla de aporte ER5356. La soldadura TIG se realiza utilizando los siguientes parámetros de diámetro del electrodo de tungsteno (2,4 mm), corriente (170 A), y caudal de gas de protección (argón) (11 l·min^{-1}). En segundo lugar, el FSP se lleva a cabo en la aleación de aluminio 5052-H32 y la aleación de aluminio 5083-H111 soldadas con TIG utilizando diferentes velocidades de rotación de la herramienta (850 a 1050 rpm), velocidades transversales de la herramienta (24 a 32 mm·min^{-1}) y un número de pasadas (1 a 3) y con una herramienta sin pasador cilíndrico. Los parámetros FSP están diseñados por la matriz Taguchi L9 para calcular los parámetros optimizados. La resistencia a la tracción, la microdureza y el % se realizan para nueve muestras distintas. Finalmente, el análisis relacional gris (GRA) se emplea para encontrar el mejor parámetro FSP de entre el conjunto de parámetros FSP. Los parámetros óptimos de FSP son los siguientes: una velocidad de rotación de la herramienta de 950 rpm, una velocidad de desplazamiento de la herramienta de 28 mm/min y un número de pasadas de 3. El número de pasadas es el factor que más influye en comparación con los otros dos parámetros de FSP.

PALABRAS CLAVE: Aleaciones de aluminio; Análisis relacional gris; Ensayos de tracción; Microscopía electrónica de barrido; Soldadura por fricción-agitación; Soldadura TIG

ORCID ID: C. Chanakyan (https://orcid.org/0000-0001-6546-7726); D. Antony Prabu (https://orcid.org/0000-0003-2550-0952); S.V. Alagarsamy (https://orcid.org/0000-0002-6564-0346); M. Martin Charles (https://orcid.org/0000-0002-7861-8009)

1. INTRODUCTION

Nowadays, the firms are in the need of unconventional light-weight materials for production and fabrication with a good thermal and electrical conductivity (Praveen *et al.*, 2005). In this respect, aluminium alloys are superior materials among various types of metals and alloys, and they can be welded together by employing different techniques. The TIG welding process is a good process for the joining of aluminium alloys compared to other joining techniques (Yazdipour *et al.*, 2011). The 5XXX aluminium alloys show superplasticity and they are used in various applications such as marine, railways, automotive and aircraft sectors. These alloys possess high corrosion resistant because of the presence of magnesium in its composition and it is also used for fabricating pressure vessels (Pavan *et al.*, 2021; Mohan Kumar *et al.*, 2022). A high mechanical strength can be achieved by the TIG welding, making it suitable for various applications. The TIG welding process is very suitable for constructions and other mechanical fabrication sectors (Huang *et al.*, 2018). The mechanical properties of joining materials are mainly affected during TIG welding. The chosen TIG welding process parameters are the filler rod diameter, the shielding gas flow rate and the current. The weld zone properties are mainly influenced by the current. The optimum current exhibits better quality for welding.The other inputs like,the filler rod material, the shielding gas and the number passes influence theformation of residual stress (Pawan *et al.*, 2013; Senthil kumar *et al.*, 2007). The defects that occurred in the welded specimen are mainly due to poor parameters selection. The defects are undercuts, scarce penetration of weld joints and unseemly weld surface. The temperature is the main factor for obtaining good quality welds and it is main influencing factor of the microstructure of the weld (Correa *et al.*, 2009; Ambriz *et al.*, 2010; Rojas *et al.*, 2020). Durgutlu (2016) studied the TIG welding technique on an aluminium silicon alloy using different process parameters. They performed mechanical tests to investigate the weld strength. The influence of the alternative and pulsed currents was analyzed and the alternative current exhibits maximum strength. Samiuddin *et al.* (2021) investigated the TIG welded 5083 alloy to analyze the microstructure and the mechanical performance for cryogenic applications. Most of the mechanical properties showed defect free joints. Gulshan and Ahsan (2014) analysed the TIG welding input parameters of aluminium alloy 1XXX for mechanical properties. In this investigation, the bonding structure and mechanical properties were analysed by utilizing the proper equipment. It was found that higher values of the heat input parameter led to better mechanical properties. Chawinee *et al.* (2010) investigated the quality of the modified surface after using the TIG welding method to join a mild steel and 5052 aluminium alloy. The inclusion and non-inclusion of oxide layers was analysed. The presence of the oxide layer produced better quality surfaces. Chanakyan *et al.* (2020) used three tool pin to predict the optimum process parameters of Friction Stir processing while joining 5052 aluminium alloys with each other. The optimum process parameters exhibited superior mechanical properties. Elmariung *et al.* (2021) analysed the TIG welding of an Inconel alloy by considering the voltage, the current and the speed parameters. The selected parameters exhibit the best mechanical properties with minor defects and this was confirmed by the microstructural study.

Chanakyan *et al.* (2021b) optimized the FSP parameters with the Taguchi approach and the ANOVA method. This approach is found useful to select the best parameters to get optimum mechanical properties. Jagathesh *et al.* (2017) analyzed the tensile properties of FSW aluminium alloy 2024 and aluminium alloy 6061 using various input factors like the spinning speed, the diameter of tool pin and the traverse speed. The optimized parameters are determined by using the Taguchi based response surface methodology. Chanakyan and Sivasankar (2020) also studied a numerical based analysis on various investigations. These studies found this approach as a very capable analysis method to obtain better optimum process parameters of FSP related studies. The FSP is a solid state joining technique that aims to obtain joints with optimum mechanical properties.

In this study, the process parameters of the TIG welding are optimized by using various techniques and the mechanical characteristics of the TIG welded joints are analysed. Besides, the input parameters of the FSW process are also optimized by using various techniques and the mechanical properties of the resulting FSP welded microstructures are also analysed. In the literature, there is no previous attempt made on the optimization of FSP parameters of TIG butt welded AA5053-H32 and AA5083 – H111 aluminium alloy with regards to the UTS, Vickers hardness and % of elongation. In this research, the TIG welding of AA5052-H32 with AA5083 – H111 alloy is carried out. The input parameters of the FSP on TIG welded bead of aluminium alloy 5052-H32 and aluminium alloy 5083 – H111 are optimized to obtain the optimum UTS, Vickers hardness and % of elongation.

2. EXPERIMENTATION

2.1. Materials

The joint efficiency of the TIG welded AA5052-H32 was 60% even though the AA5052-H32 alloy possesses a UTS of 241 MPa. The joint efficiency of the any welded metal is low compared to the base metal strength. So there is a need to increase the joint's strength. The best method to increase the joint strength of metals is the welding of a weaker metal with a stronger one (Antony Prabu and Kumarasamy, 2021). In this investigation, to increase the joint efficiency of the AA5052-H32 during TIG welding, the AA5083-H111 strong metal was chosen. The tensile strength of the AA5083 is 330 MPa. The dissimilar alloys AA5052-H32 and AA5083-H111 were welded using optimized TIG welding process parameters.

The Energy Dispersive Analysis is used for the analysis of the presence of elements in the A5052-H32 and AA5083-H111 base metals. The EDAX test result of AA5052-H32 shows that it has the following composition (in wt.-%) 0.388Fe-2.48Mg-0.19Cr-0.092Cu-0.092Mn-0.092Si-0.008Zn-0.03Ti with Al to balance. Besides, the EDAX test result of AA5083-H111 shows the following composition (in wt.-%) 0.259Fe-4.254Mg-0.113Cr-0.346Cu-0.525Mn-0.980Si-0.002Zn-0.019Ti with Al to balance. The ER5356 filler rod was employed for this investigation. The chemical composition of ER5356 is 0.4Fe-5Mg-0.25Si-0.19Cr-0.150Mn-0.1Cu-0.14Ti-0.10Zn with Al to balance. The ER5356 filler material with 2.4 mm diameter is chosen based on literature survey.

2.2. Fabrication method

The AA5052-H32 and AA5083-H111 alloys were used with dimensions of 150×55×5 mm. Each welding specimen was notched to 45° by using the Wire cut EDM. The specimens were cleaned by using silica sheets and alumina paste before welding. The Miller – Syncrowave power source were employed for TIG welding of AA5052-H32 and AA5083-H111 alloys. The ER5356 filler rod, a current of 170 amps, a shielding gas flow rate of 11 $l \cdot min^{-1}$ and a diameter of filler rod of 2.4 mm were employed for the TIG welding of the proposed aluminium alloys. The shielding gas selected for this investigation was argon. To enhance the joint efficiency, the application of the secondary process was needed on the TIG welded specimen. The secondary process consisting in using the Friction Stir Processing (FSP) with pin less tool with dimension of 40 mm of shoulder length, with 20 mm diameter of shoulder. In this research, the optimization of the FSP process parameters on the TIG welded AA5052-H32 and AA5083-H111 alloys was done by utilizing the Taguchi based GRA approach. The selected input parameters used in the FSP were the total travel speed, the total rotation speed and the number of passes. The schematic layout of FSP is shown in Fig. 1. The processed specimen is exhibited in Fig. 2.

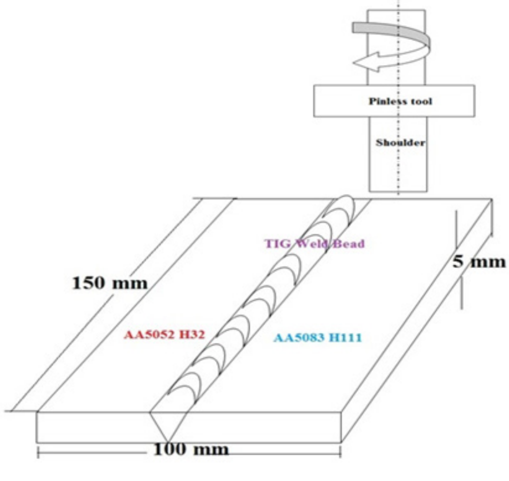

Figure 1. Configuration of FSP applied on the TIG butt welded joints using a pin less tool.

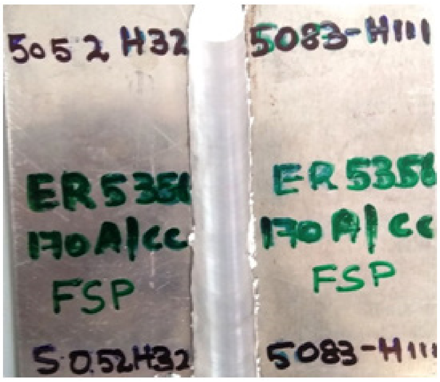

Figure 2. Friction stir processed on TIG welded sample.

The factor ranges considered in the selection of The FSP parameters are displayed in Table 1. The L9 OA was chosen for the optimization. Table 2 presents the L9 array with the different input FSP parameters considered for each sample.

Table 1. Factor ranges considered in the selection of the FSP parameters

Parameters	Abbreviation	Factors		
		1	2	3
Tool rotation speed (RPM)	X (TR)	850	950	1050
No of passes	Z (NP)	1	2	3
Tool travel speed (mm/min)	Y(TT)	24	28	32

Table 2. L9 OA with Friction Stir Processing (FSP) parameters

Sample Nº	Tool rotation speed	Tool Transverse speed	Nº of passes
1	850	24	1
2	850	28	2
3	850	32	3
4	950	24	2
5	950	28	3
6	950	32	1
7	1050	24	3
8	1050	28	1
9	1050	32	2

2.3. Testing of FSP processed TIG welded aluminium alloys 5052-H32 and 5083-H32 alloys

The AA5052-H32 and AA5083-H32were TIG welded according to the L9 orthogonal array of FSP parameters (Table 2) and tensile and Vickers hardness test were conducted accordingly. The FSP processed TIG welded specimens for the tensile testing were produced according to ASTM E8Mstandard. Wire cut EDM was utilized to cut the FSP processed TIG welded specimen. The FSP processed weld portion of the TIG welded specimen was fully incorporated in the tensile test specimen. INSTRON 8802 MTL tensile test equipment was utilized to conduct tensile tests and the strain rates 1 x 10^{-3} s^{-1} at room temperature is maintained for all the specimens. The tensile specimen with dimensions of 32 mm of gauge length, with 6 mm of width, with 30 mm of grip length, with 10 mm of grip width and with 25 mm of reduced section length. The percentage of elongation was determined after conducting the tensile tests. The Vickers hardness examination was done on the weld bead of every FSP processed with TIG welded sample by employing a Shimadzu HMV-2 Digital Vickers Hardness Tester. The Vickers hardness test was conducted under the condition of 1 kg for 15 seconds duration. In this Vickers hardness test, all the hardness values were taken on the stirred zone of dissimilar welded joints. Three trials were performed and the average value has been determined for the ultimate tensile strength (UTS), the Vickers hardness and the % of elongation. The responses selected for the optimization are the UTS, Vickers hardness and percentage of elongation. The tensile test specimens were subjected to a microstructure and fractography analysis by utilizing Scanning Electron Microscopy.

3. RESULTS AND DISCUSSION

The optimization of the input parameters of FSP on TIG welded AA5052-H111 and AA5083-H32 alloys were done by utilizing the Grey Relational Approach (GRA) approach. The L9 orthogonal arrays input parameters and its responses are mentioned in Table 3. Three trials were carried out for every combination of L9 orthogonal array parameters and the average value of each response parameters has been taken.

The GRA was employed for the computation of the optimal FSP parameters for UTS, Vickers hardness and % of elongation. The following four steps were utilized in the optimization: normalization matrix, finding of Grey Relational Coefficient, finding of Grey Relational grade and finding of rank, for every combination of FSP parameters of the L9 orthogonal array. Table 4 shows the GRA with L9 orthogonal array FSP parameters.

GRA methodology is the best optimization tool for multiple responses and it is also named as multi objective tool for optimization. The normalized matrix, GRC, GRG and ranks were determined for L9 array of FSP parameters of TIG welded dissimilar aluminium alloys. The Trail no.5 exhibits better responses among the L9 trials. The GRG value of L9 combination of parameters was compared with each other and it is shown in Fig. 3. The highest GRG value was obtained from trial no. 5.

Table 3. Mechanical properties with L9 FSP parameters

Sample N°	Tool rotation speed	Tool Transverse speed	N° of passes	Tensile Strength	Micro hardness	% El
1	850	24	1	147	76	13.2
2	850	28	2	156.3	74.3	12.8
3	850	32	3	141.9	84.9	14.0
4	950	24	2	183.54	73	15.3
5	950	28	3	191	77	16
6	950	32	1	167	73	14.77
7	1050	24	3	177	72	14.33
8	1050	28	1	163.1	78	14
9	1050	32	2	151.7	71	15.33

Table 4. Overall grey relational analysis on FSP parameters with ranking position

S. N°	Normalized S/N ratio			GRC			GRG	Rank
	Tensile Strength	Micro hardness	%El	Tensile Strength	Micro hardness	%El		
1	0.10387	0.35971	0.12500	0.35813	0.43849	0.43849	0.41170	7
2	0.29328	0.23741	0.00000	0.41435	0.39601	0.39601	0.40212	8
3	0.00000	1.00000	0.37500	0.33333	0.46801	1.00000	0.60045	2
4	0.84807	0.14388	0.78125	0.76695	0.36870	0.36870	0.50145	3
5	1.00000	0.43165	1.00000	1.00000	1.00000	0.46801	0.82267	1
6	0.51120	0.14388	0.61563	0.50566	0.36870	0.36870	0.41435	6
7	0.71487	0.07194	0.47813	0.63684	0.35013	0.35013	0.44570	5
8	0.43177	0.50360	0.37500	0.46806	0.50181	0.50181	0.49056	4
9	0.19959	0.00000	0.79063	0.38449	0.33333	0.33333	0.35039	9

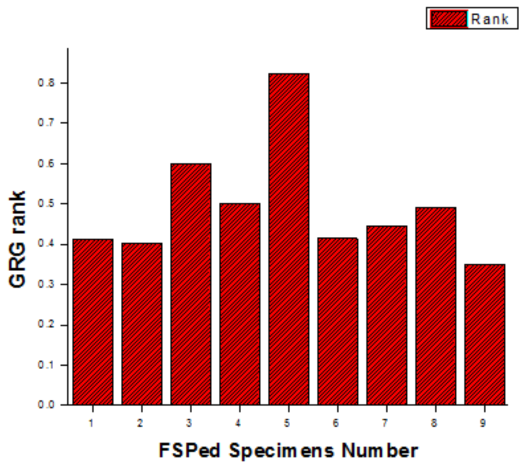

Figure 3. FSPed TIG welded runs and GRG rank.

The Grey Relational Grade was taken as the response parameter for the optimization of the FSP parameters on TIG welded dissimilar aluminium alloys. The Minitab 19 software was employed for optimization. Table 5 exhibits the response table for the GRG.

The UTS, Vickers hardness and % of elongation are significantly influenced by the number of passes, followed by total rotational speed and total transverse speed. The main interaction effect with their grey S/N ratios is illustrated in Fig. 4.

Table 5. The S/N ratios for GRG responses

Terms	Tool rotation speed (A)	Tool Transverse speed (B)	N° of passes (C)
1	-6.684	-6.908	-7.182
2	-5.114	-5.265	-7.672
3	-7.438	-7.064	-4.382
Delta	2.324	1.799	3.291
Rank	2	3	1

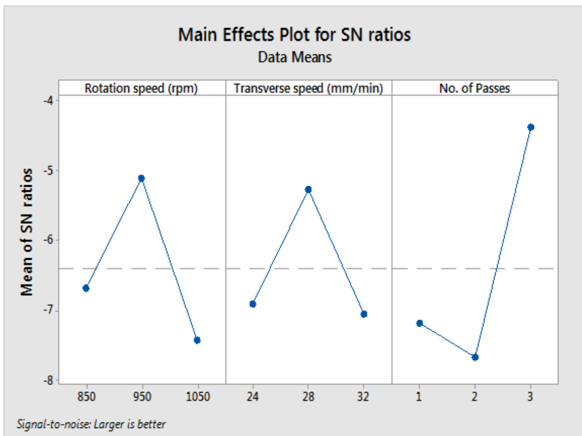

Figure 4. Main effect plot for SN ratios of GRG.

From the main effect plot, medium level of rotational and transverse speed with maximum level number of passes exhibit better UTS, Vickers hardness and % of elongation. Increasing the rotational speed increases the GRG value upto 950 rpm and then decreases at the 1050 rpm rotational speed. Increasing the transverse speed increases the GRG value upto 28 mm·min^{-1} and then decreases for 32 mm·min^{-1}. Increasing the number of passes decreases the GRG value down to 2 number of possesses and again increases the GRG value after 3 passes. Increasing of number of passes led to fine grain formation. The FSP process leads to fine grain formation on the TIG welded surface. The fine grains enhanced the mechanical properties of FSP processes TIG welded aluminium joints. The fine grain formation also increases the bonding strength between the particles of TIG welded surface. The optimized input process parameters for FSP are A2B2C3. The ANOVA for GRG is shown in Table 6. The ANOVA was utilized to analyse the importance of all input process parameters on the responses Chanakyan *et al.* (2021a). Besides, ANOVA was applied to compute the contribution percentage of each input process parameter on the GRG.

The ANOVA Table 6 shows the contribution percentage of total rotational speed; total transverse speed and number of passes are 25.8, 19.7 and 54.3%, respectively. The influencing sequences of input process parameter of FSP are the number of passes, total rotational speed and the total transverse speed. Consequently, the contour plots of various combinations of input process parameters for different responses are shown in Fig. 5(a-c).

The contour plot for the rotational speed and the transverse speed on the GRG reveals that medium level of rotational speed 950 rpm and medium level of transverse speed 28 mm/min exhibit highest the GRG value as it was shown in Fig. 5a. The Fig. 5b depicts the relationship between the transverse speed and number of passes, revealing that the highest number of passes (3) with a medium level of transverse speed enhances the GRG value. Figure 5c shows that the medium level of total rotational speed 950 rpm and 3 passes exhibit higher GRG value among the possible combinations.

The confirmation test was done for the A2B2C3 combination of input process parameters of FSP. The confirmation test specimen was TIG welded at 170 A of current, 2.4 mm diameter of filler rod and 11 l·min^{-1} gas flow rate. The filler material ER5356 was employed for the TIG welding. The TIG welded dissimilar alloy sample was further FSP processed at the condition of 950 rpm rotational speed, 28 m·min^{-1} transverse speed and using 3 passes. The two trails were done for assessing the UTS, Vickers hardness and % of elongation. The two trails were conducted for the confirmation test process parameters.

The UTS, Vickers hardness and % of elongation obtained were 246 MPa, 112 HV and 19.2%. The

Table 6. ANOVA for GRG with FSP parameters

Process parameters of FSP	DF	Seq SS	Adj MS	F	P	%
TR (rpm)	2	0.03617	0.01809	1.53	0.396	25.8
TP (mm/min)	2	0.02775	0.01387	1.17	0.461	19.7
NP	2	0.07632	0.03816	3.22	0.237	54.3
Error	2	0.02369	0.01184			0.2
Total	8	0.16393				100

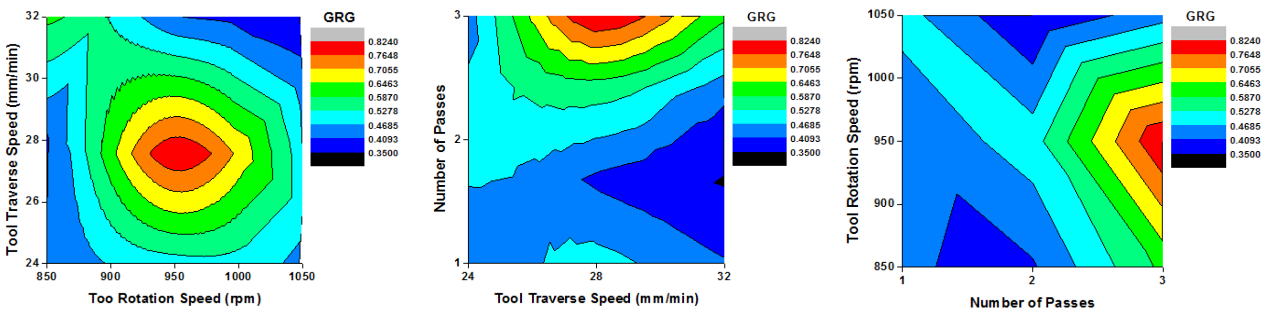

(a) (b) (c)

Figure 5. (a) Influence of the Tool Rotation and Tool Rotation Speed on the GRG; (b) Influence of the Tool Transverse Speed and Number of Passes on the GRG; (c) Influence of the Number of Passes and the Tool Rotation Speed on the GRG.

joint efficiency of the FSP processed TIG welded AA5052-H32 and AA5083-H111 are enhanced to 102.5%. The confirmation test specimen was displayed in Fig. 6 (a-b).

Figure 6. (a) Confirmation test specimen for the tensile tests; b) Confirmation test specimen for tensile test after fracture.

Scanning Electron Microscopy was employed for analysing the fracture surface of the confirmation test specimen of FSP processed TIG welded AA5052-H32 and AA5083-H111. The result is shown in Fig. 7. Porosities were formed in some places of the confirmation test specimen. Besides, oxides were formed in some regionon the fractured surfaces of the confirmation test specimen. The fractured surface reveals that ductile fracture was occurred.

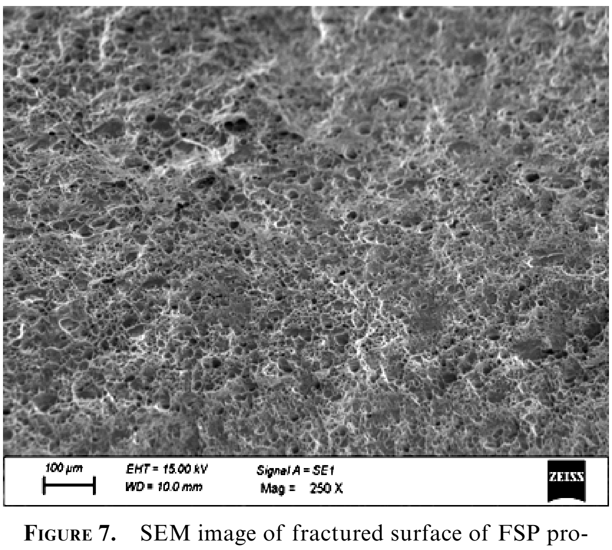

Figure 7. SEM image of fractured surface of FSP processed TIG welded AA5052-H32 and AA5083-H111 alloy (confirmation test specimen).

4. CONCLUSIONS

The TIG welding of aluminium alloy 5052-H32 and aluminium alloy 5083-H111was done at 70 A of current, 11 l·min^{-1} of gas flow rate and 2.4 mm of ER5356 filler rod material. The TIG welding dissimilar aluminium alloy sample has a low joint efficiency when compared to base metal joint strength. For this reason, the FSP was employed on the surface of the TIG welded sample. The implementation of the FSP process on the TIG welded samples was successfull, decreasing the grain size. The optimization of FSP process parameters on TIG welded TIG welded joint was done by the Grey Relational Approach (GRA). The input process parameters of the FSP process are the total rotational speed, the total transverse speed and the number of passes. Response parameters are selected for this investigation to enhance the ultimate tensile strength (UTS), Vickers hardness and % of elongation. The optimum combination of input FSP parameters was A2B2C3. The influencing parameter sequence of FSP was the number of passes, the total rotational speed and the transverse speed. Its contribution percentage for the GRG was 54.3, 25.8 and 19.7%, respectively. The microstructure of the TIG welded AA5052-H32 and AA5083-H111weld bead was analysed before and after the implementation of the FSP by using SEM. The SEM image of the fractured surface confirmation test specimen shows that there were no considerable defects and a ductile fracture. The efficiency of joint processed by a combination of FSP and TIG was increased to around 103%.

REFERENCES

Ambriz, R.R., Barrera, G., García, R., López, V.H. (2010). Effect of the weld thermal cycles of the modified indirect electric arc on the mechanical properties of the AA6061-T6 alloy. *Weld. Int.* 24, 321–328. https://doi.org/10.1080/09507110903568778.

Antony Prabu, D., Kumarasamy, S. (2021). Mechanical properties and metallurgical characterization of FSPed TIG and TIG welded AA5052-H32/AA5083-H111 dissimilar aluminium alloys. *Metall. Res. Technol.* 118 (3), 304. https://doi.org/10.1051/metal/2021005.

Chanakyan, C., Sivasankar, S. (2020). Parametric studies in friction stir welding on Al-Mg alloy with (HCHCr) tool by Taguchi based desirability function analysis (DFA). *J. Ceram. Process. Res.* 21 (6), 647-655. https://doi.org/10.36410/jcpr.2020.21.6.647.

Chanakyan, C., Sivasankar, S., Meignanamoorthy, M., Ravichandran, M., Alagarsamy, S.V., Dinesh Kumar, S., Sakthivelu, S. (2020). Friction stir processing (FSP) of numerical study based on design of experiment-review. *Mater. Today. Proceed.* 27 (2), 748-751. https://doi.org/10.1016/j.matpr.2019.12.035.

Chanakyan, C., Sivasankar, S., Meignanamoorthy, M., Ravichandran, M., Mohanavel, V., Saleh, A., Hesham, S.A., Manikandan, V., Ramesh Lalvani, J.I. (2021a). Optimization of FSP Process Parameters on AA5052 Employing the S/N Ratio and ANOVA Method. *Adv. Mater. Sci. Eng.* 2021, 6450251. https://doi.org/10.1155/2021/6450251.

Chanakyan, C., Sivasankar, S., Meignanamoorthy, M., Alagarsamy, S.V. (2021b). Parametric Optimization of Mechanical Properties via FSW on AA5052 Using Taguchi Based Grey Relational Analysis. *Incas. Bulletin* 13 (2), 21-30. https://doi.org/10.13111/2066-8201.2021.13.2.3.

Chawinee, P., Pusit, M., Tapany, U., Rattana, B. (2010). Effects of Aluminium Alloy Surface Preparation in TIG Dissimilar Metals Welding between Mild Steel and 5052 Aluminium Alloy. *Proceed. 12th. Int. Conf. Aluminium. Alloys*, Japan, pp. 961-965.

Correa, E.O., Costa, S.C., Santos, J.N. (2009). Studies on weldability of iron-based powder metal alloys using pulsed gas tungsten arc welding process. *J. Mater. Process. Technol.* 209 (8), 3937-42. https://doi.org/10.1016/j.jmatprotec.2008.09.008.

Durgutlu, A. (2016). The effect of continuous and pulsed current on microstructure and mechanical properties in TIG welding of Al-Si alloy sheets. *Kovove. Mater.* 54 (5), 345–350. https://doi.org/10.4149/km_2016_5_345.

Elmariung, A., Sivagami, S.M., Chanakyan, C., Arockiam, J., Sathishkumar, G.B., Meignanamoorthy, M., Ravichandran, M., Alagarsamy, S.V. (2021). Mechanical properties on INCONEL 800H alloy by TIG welding process. *Mater. Today. Proceed.* In Press https://doi.org/10.1016/j.matpr.2021.01.049.

Gulshan, F., Ahsan, Q. (2014). Effect of Heat Input on the Structure and Properties of Aluminium Weldment TIG Welded with 4043 Filler Rod. *Chem. Mater. Eng.* 2 (2), 25-32. https://doi.org/10.13189/cme.2014.020201.

Huang, L., Wu, D., Hua, X., Liu, S., Jiang, Z., Li, F., Wang, H., Shi, S. (2018). Effect of the welding direction on the microstructural characterization in fiber laser-GMAW hybrid welding of 5083 aluminum alloy. *J. Manuf. Process.* 31, 514-522. https://doi.org/10.1016/j.jmapro.2017.12.010.

Jagathesh, K., Jenarthanan, M.P., Dinesh Babu, P., Chanakyan, C. (2017). Analysis of factors influencing tensile strength in dissimilar welds of AA2024 and AA6061 produced by Friction Stir Welding (FSW). *Aust. J. Mech. Eng.* 15 (1), 19-26. https://doi.org/10.1080/14484846.2015.1093229.

Mohan Kumar, S., Rajesh Kannan, A., Pramod, R., Siva Shanmugam, N., Dhinakaran, V. (2022). Testing, characterization and numerical prediction (uni-axial tension and bend test) of Double-side TIG welded SS321 plate for pressure vessel application. *Int. J. Press. Vessels. Piping.* 197 (15), 104648. https://doi.org/10.1016/j.ijpvp.2022.104648.

Pavan, A.R., Chandrasekar, N., Arivazhagan, B., Kumar, S., Vasudevan, M. (2021). Study of arc characteristics using varying shielding gas and optimization of activated-TIG welding technique for thick AISI 316L(N) plates. CIRP *J. Manuf. Sci. Technol.* 35, 675-690. https://doi.org/10.1016/j.cirpj.2021.08.013.

Pawan, K., Anoop, C.A., Kumar, S. (2013). Study of Heat Input for GTA Welded Aluminium Alloy 7039. *Int. J. Eng. Sci. Innov. Technol.* 2 (5), 150-156. https://doi.org/10.13140/RG.2.2.10701.44009.

Praveen, P., Yarlagadda, P.K.D.V., Kang, M.J. (2005). Advancements in pulse gas metal arc welding. *J. Mater. Process. Technol.* 164–165, 1113-1119. https://doi.org/10.1016/j.jmatprotec.2005.02.100.

Rojas. H., Molina, A., Valdez, S., Campillo, B., Martínez H., Sedano, A., Serna, S. (2020). The impact of heat input on the microstructures, fatigue behaviors, and stress lives of TIG-welded 6061-T6 alloy joints. *Mater. Res. Express.* 7, 126512. https://doi.org/10.1088/2053-1591/abd136.

Samiuddin, M., Li, J., Taimoor, M., Nouman Siddiqui, M., Siddiqui, S.U., Xiong, J. (2021). Investigation on the process parameters of TIG-welded aluminum alloy through mechanical and microstructural characterization. *Def. Technol.* 17 (4), 1234-1248. https://doi.org/10.1016/j.dt.2020.06.012.

Senthil Kumar, T., Balasubramanian, V., Babu, S., Sanavullah,M.Y. (2007). Effect of Pulsed Current GTAW Parameters on Fusion Zone Microstructure of AA6061 aluminium alloy. *Met. Mater. Int.* 13, 345-351. https://doi.org/10.1007/BF03027892.

Yazdipour, A.R., Shafiei, M., Jamshidi Aval, H. (2011). An investigation of the microstructures and properties of metal inert gas and friction stir welds in aluminium alloy 5083. *Sadhana* 36, 505-514. https://doi.org/10.1007/s12046-011-0032-6.